Eur. Phys. J. B **75**, 443–450 (2010)
DOI: 10.1140/epjb/e2010-00155-9

THE EUROPEAN PHYSICAL JOURNAL B

Regular Article

Thermodynamics of the rupture in a Morse lattice

V.N. Likhachev[1], T.Yu. Astakhova[1], W. Ebeling[2], M.G. Velarde[3], and G.A. Vinogradov[1,a]

[1] Emanuel Institute of Biochemical Physics, Russian Academy of Sciences, ul. Kosygina 4, 119334 Moscow, Russian Federation
[2] Institut für Physik, Humboldt-Universität Berlin, Newtonstrasse 15, 12489 Berlin, Germany
[3] Instituto Pluridisciplinar, Universidad Complutense de Madrid, Paseo Juan XXIII, 1, 28040 Madrid, Spain

Received 20 December 2009 / Received in final form 11 March 2010
Published online 19 May 2010 –

Abstract. The rupture of a Morse lattice is considered in the present paper. The critical rupture force F_{cr} is found to decrease with the number of particles N as $F_{cr} \sim 1/\sqrt{N}$. The partition function is obtained for two states of the lattice – with all equal bond lengths and one broken bond. In the first case an accurate expressions for thermodynamic parameters are obtained, and thermodynamic expressions are derived in the harmonic approximation in the latter case. The analytical predictions are confirmed by extensive MD simulations. Cis-trans isomerization is considered as an example. Volume fractions of trans- and cis-isomers versus number of monomer units N are found depending on the torsion stiffnesses.

1 Introduction

In a recent work [1] we developed general methods for the treatment of thermodynamic processes in one-dimensional nonlinear systems. Here we will give an application to a special problem of high interest, – rupture of polymeric and biological macromolecules. The problem of macromolecule rupture and hence an irreversible transition in macromolecule form and eventually function is of relevance for many biological and technical processes. Polymer molecules can be broken by different reasons: stretching [2–4], surface adsorption [5], in elongational flows [6–10], etc. On the other hand, typical irreversible transitions in biological systems occur due to: mechanical failure of enzymes [11], rupture of the enzyme-inhibitor interaction [12], dissociation of a biomolecular complex [13], or conformational transformations in elastic biopolymers at stretching [14].

A variety of methods are used to understand the rupture dynamics of homopolymers: classical [15–17], steered [18], and ab initio [19] molecular dynamics (MD) as well as Monte Carlo [20–22] in combination with different analytical investigations [16,22–24]. Two-dimensional lattices with bond disorder were also used to investigate the fracture behaviour under stress-controlled conditions [25,26].

Reversible transitions in polymers are also possible. Examples are morphological switches of reversible imine bonds [27], phase transition between two equilibrium states of polymer chains [28,29], coil-to-globule transition [30], reversible cross-linking and splitting of polymer networks formed in two strain states [17]. Biopolymers are often in equilibrium between two states: equilibrium of two conformational states of a polysaccharide molecule [14], two pathways of a structural relaxation of DNA in solution [31]. See for recent reviews on bond rupture in artificial [32,33] and natural [34–36] macromolecules.

Complex polymer and biological objects are often modelled by using simple interaction potentials, and one of most familiar is the Morse potential [23,37–39]. The lattice rupture is most commonly investigated under a constant loading rate in a time-varying one-dimensional potential well in the presence of thermal fluctuations for evaluating the escape time for the transition to the state with one broken bond [23,37,38]. The analysis is performed using both the Kramers escape theory [40,41], thermally activated processes in non-linear polymer dynamics [42] and MD simulation. In the latter case it has been shown that the cubic theory for Morse potential [37] gives better results, and the rupture force scales $\propto -[\ln(\text{const}R)]^{2/3}$ where R is the loading rate. This approach was generalized for the case of arbitrary particle number in a homogeneous chain [43] obtaining the most probable rupture force $F_{\max} \propto -\ln[(\text{const}\, N/R]^{2/3}$ that finally approaches a saturation value independent on N. Other approach is associated with the reconstructing the potential energy landscape of simple polypeptidic chains [44,45]. It allows an effective estimations of the time scales associated with both folding and equilibration processes.

Lattice rupture is possible at considerable deformations or high temperatures in the Morse lattice. Some results are known about the thermodynamics of this system [46,47]. Analogous problems were also analyzed in references [48–50] where mechanisms and different structure types were considered.

[a] e-mail: gvin@deom.chph.ras.ru

2 Rupture of the Morse lattice

The Morse potential for the interaction of nearest-neighbor particles with masses m can be written as [43]:

$$u(l_i) = \frac{C}{2\alpha}[1 - \exp(-\alpha\, l_i)]^2\,, \tag{1}$$

where $C/2\alpha$ is the potential well depth (binding/dissociation energy), $1/\alpha$ characterizes the potential well width, $l_i = (x_i - x_{i-1})$ relative deviations of particles from their equilibrium positions. We shall consider as scales of the problem the mass $[m]$, the energy $[E] = C/2\alpha$ and the length $[L] = 1/\alpha$. Typical experimental parameter values for polymers are $C/(2\alpha) = 3.5 \times 10^{-12}$ erg with $\alpha = 10$ nm^{-1} [51]. Thus for universality in the argument we shall use the dimensionless Morse potential

$$u(l_i) = [1 - \exp(-l_i)]^2\,, \tag{2}$$

where all parameters, by convention, are rescaled to the value unity. Then additional units of time and force are $[t] = \sqrt{2m/(C\alpha)}$, $[F] = C/2$, respectively. Temperature is also measured in energy units $[T] = C/(2\alpha)$ (by appropriately setting $k_{\rm B} = 1$).

We shall consider the thermodynamics of the one-dimensional (1D) Morse lattice with N particles such that $L \equiv \sum_{i=1}^{N+1} l_i$. Fixed boundary conditions $x_0 = 0$ and $x_{N+1} = L$ ensure constant lattice length L. $\varepsilon = L/(N+1)$ is the specific elongation (absolute elongation of one bond when all $N+1$ bonds have equal lengths; $\varepsilon = 0$ in the absence of deformation). The total potential energy is the sum of $(N+1)$ bond energies, including the interaction with the boundaries

$$U = u(x_1) + u(x_2 - x_1) + \ldots + u(x_N - x_{N-1}) + u(L - x_N). \tag{3}$$

All bonds have equal lengths at $T = 0$: $x_i^0 - x_{i-1}^0 = \ell_0$.

The thermodynamics will be considered for two states of the lattice, – with all equal bond lengths, where accurate expressions can be obtained, and for the state with one broken bond where thermodynamics can be described in the low temperature harmonic approximation.

2.1 Equilibrium thermodynamics of the Morse lattice in canonical ensemble

We start from the thermodynamic analysis of the lattice when it has all equal bond lengths. The equilibrium thermodynamics of systems with small number of particles has been studied using both the canonical and the microcanonical ensembles [52–55]. We focus here on the thermodynamics of one-dimensional Morse lattice (for the analogous problem in the microcanonical ensemble see [56]).

There are two ways to analyze the thermodynamics of 1D systems: one is using the (L, T, N) ensemble and the other the (F, T, N) ensemble ((V, T, N) and (P, T, N) ensembles for 3D systems). Let us show that these two ensembles give different results for finite N due to the possibility of lattice rupture. If the (F, T, N) ensemble is used and $T \to 0$ then the lattice has all equal bond lengths if the force F is less then some critical value $F^{\#}$, corresponding to the lattice rupture, and it has one broken bond if $F > F^{\#}$. In the case of (F, T, N) ensemble the bond lengths are independent of N because force F ensures constant specific elongation ε and results for finite N and for the thermodynamic limit $N \to \infty$ coincide. Using the (L, T, N) ensemble these results differ as we show below. It is more convenient to use the (ε, T, N) ensemble instead of (L, T, N) with $\varepsilon = L/(N+1)$ accounting for relative lattice extension.

The total partition function Z can be written [57] as the product $Z = Z_{\rm v} Z_{\rm x} = \int d\Gamma_{\rm x} \exp(-\beta U_{\rm p}) \int d\Gamma_{\rm v} \exp(-\beta U_{\rm k})$, where $\beta = 1/T$ (in dimensionless units such that $m = k_{\rm B} = h = 1$); $U_{\rm p}, U_{\rm k}$ are potential and kinetic energies, $d\Gamma_{\rm x} = \prod_{i=1}^{N} dx_i$, $d\Gamma_{\rm v} = \prod_{i=1}^{N} dv_i$. The partition function is $Z_{\rm v} \equiv (2\pi/\beta)^{N/2}$ in the canonical ensemble for 1D systems and gives a trivial contribution to the total partition function Z.

Following the Toda's approach [58], the partition function $Z_{\rm x}$ can be represented as a single integral and the real Fourier transformation is usually used. But it is more convenient to utilize the complex function

$$f(z, \beta) = \int \exp[-zw - \beta u(w)]\, dw; \quad (z = x + iy), \tag{4}$$

where $u(w) = [1 - \exp(-w)]^2$ is the dimensionless Morse potential (2). After a series expansion of $\exp[-\beta u(w)]$ in (4) we get

$$f(z, \beta) = \frac{\exp(\varepsilon z - \beta)}{2\,\beta^{z/2}} \sum_{k=0}^{\infty} \Gamma\left(\frac{z+k}{2}\right) \frac{(2\sqrt{\beta}\,)^k}{k!}\,, \tag{5}$$

where $\Gamma(\ldots)$ is the gamma-function of complex argument. Then $Z_{\rm x}$ reads

$$Z_{\rm x} = \frac{1}{2\pi i}\, {\rm Im} \int [f(z, \beta) \exp(\varepsilon z)]^{N+1}\,. \tag{6}$$

Note that (5) is a power series in the inverse temperature β and using this expression is of doubtful validity in the limit $T \to 0$. The computations at low temperatures should be done in the harmonic approximation.

Recalling that the potential energy $\langle U_{\rm p} \rangle = -\partial \ln Z_{\rm x}/\partial\beta$ (angular brackets stand hereafter for the corresponding ensemble average) one gets

$$\langle U_{\rm p} \rangle = -\frac{1}{Z_{\rm x}} \frac{N+1}{2\pi i}\, {\rm Im} \int \frac{\partial f(z, \beta)}{\partial \beta} \exp(\varepsilon z)\, [f(z, \beta) \times \exp(\varepsilon z)]^{N+1}\, dz\,. \tag{7}$$

An expression for the entropy can be obtained as follows. The free energy is $A = -T \ln Z$. From the thermodynamic identity $A = \langle U \rangle - TS$ one gets: $S = (\langle U_{\rm p} \rangle + \langle U_{\rm k} \rangle)/T + \ln Z_{\rm x} + \ln Z_{\rm v}$. For 1D systems in canonical ensemble $\langle U_{\rm k} \rangle \equiv NT/2$. Thus, omitting unessential numerical additional terms, the expression for the entropy reads

$$S = \langle U_{\rm p} \rangle / T + \ln Z_{\rm x} + N(\ln T)/2, \tag{8}$$

and the substitution of (6) and (7) in (8) allows to find the entropy.

The force acting on the right lattice end is defined as $\langle F\rangle = \beta^{-1}\, d(\ln Z_{\rm x})/dL$ and differentiating the partition function, one gets:

$$\langle F\rangle = \frac{1}{Z_{\rm x}}\,\frac{T}{2\pi i}\,{\rm Im}\int z[f(z,\beta)\exp(\varepsilon z)]^{N+1}\,dz. \qquad (9)$$

The integrals (6)–(9) can be calculated numerically along any line $\mathrm{Re}\, z = x > 0$ in the complex plane. But the integrand oscillates in the general case what makes the calculations inefficient and inaccurate. The optimal integration path goes through the saddle point where the integrand has Gaussian shape thus making the integration more efficient. The saddle point lies on the line $\mathrm{Re}\, z = x_0$ where x_0 is the solution of the transcendental equation

$$f'(z,\beta) + \varepsilon f(z,\beta) = 0, \qquad (10)$$

and hence x_0 depends on ε and β. Some technical problems associated with the usage of complex function (5) are compensated by considerable increase of accuracy.

The integration in all expressions above in the limit $N \to \infty$ is reduced to the calculation of integrands at the saddle point x_0 (and this is one more advantage of the usage the complex function (4)). Then for the specific potential energy $\mathcal{E}_{\rm p} = \langle U_{\rm p}\rangle / N$ we have

$$\mathcal{E}_{\rm p} = \frac{\partial}{\partial\beta}\ln\left[f(x_0,\beta\right]. \qquad (11)$$

The force (9) can be rewritten as

$$\langle F\rangle = Tx_0 - \frac{1}{Z_{\rm x}}\,\frac{T}{2\pi i}\int\limits_{-\infty}^{\infty} y\,{\rm Im}\left\{[f(z,\beta)\exp(\varepsilon z)]^{N+1}\right\} \times dy;\ (z = x_0 + iy) \qquad (12)$$

and (12) is reduced to $\langle F\rangle = Tx_0$ in the thermodynamic limit $N \to \infty$.

The specific heat at constant length c_L can be obtained by the differentiating (analytical or numerical) the expression (11) for potential energy.

The force and specific heat *versus* temperature are shown in Figures 1, 2. Analytical expression (12) for the force was examined in numerical MD simulation and very good coincidence was observed. Force acting on ith particle is $F_i = \partial U/\partial x_i$ and U is the total potential energy (3). Numerically force was calculated as the mean value $\langle F\rangle_\tau = (N\tau)^{-1}\int_0^\tau \sum_{i=1}^N F_i(\tau)$ on MD trajectory with time $\tau = 10^5$. Specific heat capacity shown in Figure 2 also coincides with good accuracy with the results obtained by numerical differentiating of potential energy in reference [59] for $\varepsilon = 0$.

If ε = const. ($\varepsilon_0 = 0.1$ for illustration) then there exists such lattice length $N^{\#}$ in the (ε, T, N) ensemble that the state with equal bonds is the ground state at $N < N^{\#}$ and the force at $T \to 0$ is equal to its static value $\langle F\rangle_{\rm st} = -2\exp(-\varepsilon_0)\left[1 - \exp(-\varepsilon_0)\right] = -0.1722$ Negative

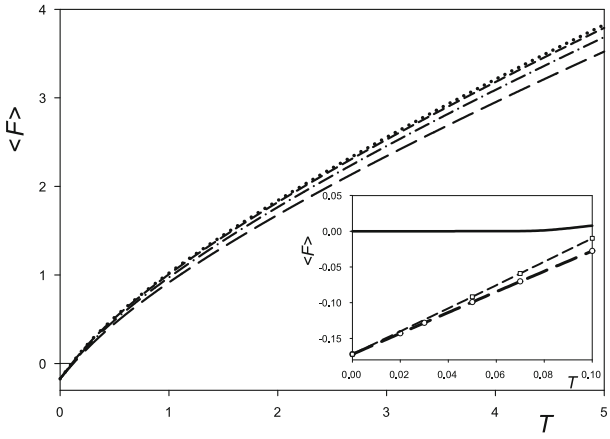

Fig. 1. Force $\langle F\rangle$ versus temperature for different number of particles: $N = 10$ (long-dash line), $N = 20$ (medium-dash line), $N = 50$ (short-dash line), $N = 100$ (dotted line), $N = \infty$ (solid line). Inset: the same at low temperatures. Symbols show the calculated values in MD simulation; standard errors are comparable with the symbol sizes. $\varepsilon = 0.1$.

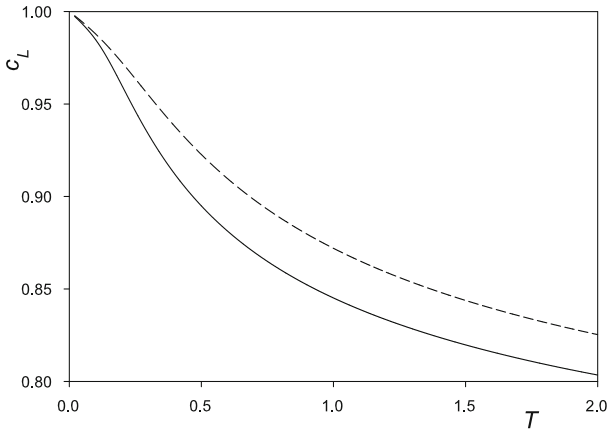

Fig. 2. Specific heat (at constant length) versus temperature for two values of ε: $\varepsilon = 0$ (solid line), $\varepsilon = 0.1$ (dashed line).

value of $\langle F\rangle_{\rm st}$ means the elongated state of the lattice. The temperature increase results in an increase of the force ("thermal expansion" – see insert to Fig. 1).

The expressions for the thermodynamic functions appear simpler in the (F, T, N) ensemble where no problems with the lattice rupture appear. Recall that specific thermodynamic parameters do not depend on N in this case and coincide with thermodynamic limit $N \to \infty$.

An expression for the potential energy in (F, T, N) ensemble is obtained by replacing the last term $u(L - x_N)$ in (3) by Fx_N. The partition function Z_x is calculated analogously to what was done above in (L, T, N) ensemble. Z_x is expressed through the complex function (4)

$$Z_x = [f(y,\beta)]^N, \qquad \text{where}\quad y = F\beta. \qquad (13)$$

The specific deformation ε at fixed force is defined by

$$\frac{\partial f(y,\beta)}{\partial y} + \varepsilon\, f(y,\beta) = 0. \qquad (14)$$

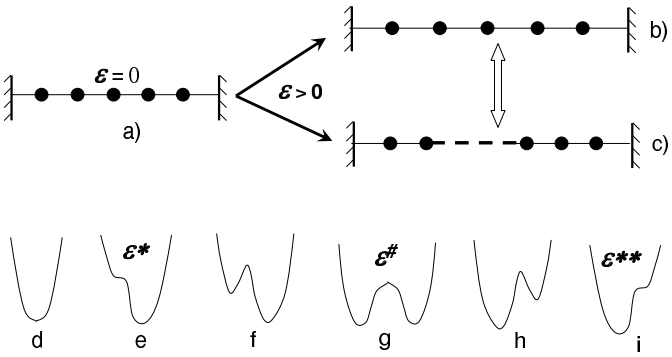

Fig. 3. Morse lattice. Upper panels: (a) lattice in the ground state at $\varepsilon = 0$; (b) lattice at $\varepsilon > 0$ with all equal bond lengths; (c) lattice at $\varepsilon > 0$ with one ruptured bond and other bonds in equilibrium. Lower panels schematically show lattice energies at different rates of deformation ε increasing from left to right: (d) lattice in relaxed state at $\varepsilon = 0$; (e) state with one ruptured bond (left potential well) appears at some specific elongation ε^*; (f) two states of the lattice with equal bond lengths and one ruptured bond; (g) equal energies of two states at $\varepsilon^{\#}$; (h) a state with one ruptured bond is energetically preferable; (i) instability at $\varepsilon^{**} \geq \ln 2 \approx 0.69$.

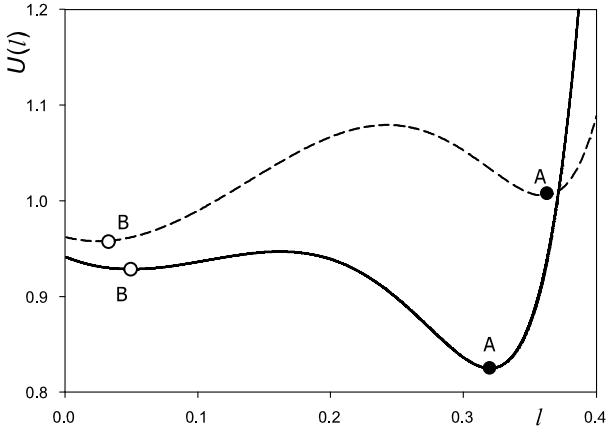

Fig. 4. Morse lattice. Potential energy U versus reaction coordinate ℓ (varying bond lengths of one bond) in the lattice of $N = 10$ particles. Upper dashed line: $\varepsilon = 0.36$, lower solid line: $\varepsilon = 0.32$. Right minima (solid circles marked with letter 'A') correspond to equal bond lengths ℓ_0, left energy minima $\widetilde{U}$ (open circles marked with letter 'B') – N bonds have length ℓ_1, and one bond – length ℓ_2. Energy increase of the state with $\varepsilon = 0.36$ in comparison with $\varepsilon = 0.32$ is due to work of external forces on lattice elongation. Energy unit $[E] = C/(2\alpha)$ of potential (1).

This expression formally coincides with (10) but now is not a transcendental equation, but the equation in ε. The specific potential energy $\langle U_{\rm p}\rangle / N$ is

$$\mathcal{E}_{\rm p} = -f'_{\beta}(y,\beta)/f(y,\beta). \tag{15}$$

The specific heat at constant force c_F is obtained by differentiating the specific potential energy (15)

$$c_F = \beta^2 \left(\frac{f''_{\beta\beta}}{f} + \frac{f''_{y\beta}}{f} F - \mathcal{E}_{\rm p}^2 - \varepsilon\, \mathcal{E}_{\rm p} f \right). \tag{16}$$

In contrast to the expression for the specific heat c_L at constant length, where the second derivative of the gamma-function appears, (16) is represented through an analytical series.

2.2 Lattice rupture

An overview of possibilities offered by the lattice as we vary ε from its zero value up are shown in Figure 3. If $\varepsilon < \varepsilon^{\#}$ then the state with equal bond lengths is the ground state, in the opposite case ($\varepsilon > \varepsilon^{\#}$) the state with one broken bond is energetically favorable. Reversible transitions between both states are possible under the influence of thermal fluctuations.

Lattice parameters (energy, bond lengths, forces) at critical values $\varepsilon^*, \varepsilon^{\#}, \varepsilon^{**}$ of the specific deformation are determined by searching for the stationary points of the potential energy, i.e. $\partial U/\partial \ell = 0$ (ℓ is equilibrium bond length). For the lattice with one broken bond it can be done in the simple case where first N bond lengths are ℓ_1 and the last broken bond has length $\ell_2 = L - N\ell_1$. The equilibrium coordinates of particles when the $(N+1)$th bond breaks are: $x_i^0 = i\,\ell_1$, $(i = 1, 2, \ldots, N)$ and $x_{N+1}^0 =$ L. $(N+1)$ possibilities exist as any of the bonds can be broken.

The transition (see Fig. 3f) from the right minimum (equal bond lengths ℓ_0) to the left minimum (one broken bond with length ℓ_2 and N bonds with lengths ℓ_1) of the total potential energy can be considered as the "reaction coordinate" when any bond changes its length from ℓ_0 to ℓ_2 with the corresponding rearrangement of the other bond lengths. If the ground state is the state with one broken bond then N bond lengths l_i fluctuate around ℓ_1 and one around ℓ_2, and the potential energy is $\widetilde{U} = \sum_{i=1}^{N} u(l_i) + u(L - \sum_{i=1}^{N} l_i)$ ('tilde' is used hereafter to account for the lattice parameters when there is one broken bond).

Accurate values of potential energies are shown in Figure 4 for two values of ε. The horizontal axis is the "reaction coordinate" i.e. the length of a breakable bond. One can see that the state with equal bond lengths ℓ_0 is the ground state for $\varepsilon = 0.32$, but when $\varepsilon = 0.36$ the ground state is with one broken bond. For $\varepsilon = \varepsilon^{\#}$ in the range $0.32 < \varepsilon < 0.36$ there is degeneracy as both energy minima are at equal depth.

For $\varepsilon > \varepsilon^*$ the energy minimum corresponds to the lattice with one broken bond. To obtain all lattice parameter values (bond lengths, energy and force) when $\varepsilon = \varepsilon^*$ we can use the functional

$$\Phi = N u(\ell_1) + u(\ell_2) + \mu\,(N\ell_1 + \ell_2)\,, \tag{17}$$

where μ is a Lagrange multiplier. Solving the corresponding variational equations

$$\frac{\partial \Phi}{\partial \ell_1} = 0; \qquad \frac{\partial \Phi}{\partial \ell_2} = 0; \qquad \frac{\partial \Phi}{\partial \mu} = N\ell_1 + \ell_2, \tag{18}$$

we get ℓ_1 and ℓ_2:

$$\ell_{1,2} = -\ln\left[\frac{1}{2}\left(1 \pm \sqrt{1+2F}\right)\right]. \tag{19}$$

The plus sign in (19) corresponds to equal bond lengths ℓ_1 of N unbroken bonds, and the minus sign to the length of broken bond ℓ_2. The Lagrange multiplier μ is actually the force $F = -u'(\ell)$ such that

$$F = 2[\exp(-\ell_{1,2}) - 1]\exp(-\ell_{1,2}). \tag{20}$$

Using $\ell_{1,2}$ (19) in equation (20) permits obtaining F. The specific elongation $\varepsilon^* = L^*/(N+1)$ and the corresponding force F^* at the "critical" point ε^* are

$$\varepsilon^* = [N\ln N - \ln(N+1)]/(N+1)^2;\ F^* = 2N/(N+1)^2. \tag{21}$$

For long lattices ($N \to \infty$), $\varepsilon^* \sim \ln N/N$ and $F^* \sim 2/N$. Three solutions of system (18)–(20) exist when $\varepsilon > \varepsilon^*$: two correspond to energy minima for states with equal bond lengths and one broken bond, and the third to the barrier separating two energy minima.

The energy minima of the ground states with equal bond lengths U_g and one broken bond $\widetilde{U}_g$ are given by $U_g = (N+1)[1-\exp(-\ell_0)]^2$ and $\widetilde{U}_g = N[1-\exp(-\ell_1)]^2 + [1-\exp(-\ell_2)]^2$, respectively. U_g is the ground state when $\varepsilon < \varepsilon^{\#}$ and $\widetilde{U}_g$ for $\varepsilon > \varepsilon^{\#}$. If the barrier separating two energy minima is not high enough (when $\varepsilon \approx \varepsilon^{\#}$), then the lattice is in the "mixed" state and transitions between broken state and the state with all equal bond lengths are possible.

The lattice parameter values when $\varepsilon = \varepsilon^{\#}$ are also defined by (19)–(20) and $\varepsilon^{\#} = -\ln[1-(N+1)^{-1/2}]$ and $\varepsilon^{\#} \sim 1/\sqrt{N}$ and $F^{\#} \sim 2/\sqrt{N}$ for $N \to \infty$. The force value $F_{cr} = F^{\#}$ is the critical force for lattice rupture.

Figure 5 shows ε^* and $\varepsilon^{\#}$ versus N. When $N \to \infty$ the lattice is unstable to the rupture at an arbitrary small but finite $\varepsilon > 0$ and the only problem is how the rearrangement kinetics may take place.

One more "critical" point is ε^{**}, i.e. the point of absolute instability (see Fig. 3i). This value is determined from the condition that the second derivative of u changes sign, thus leading to $\varepsilon^{**} = \ln 2 \approx 0.69$.

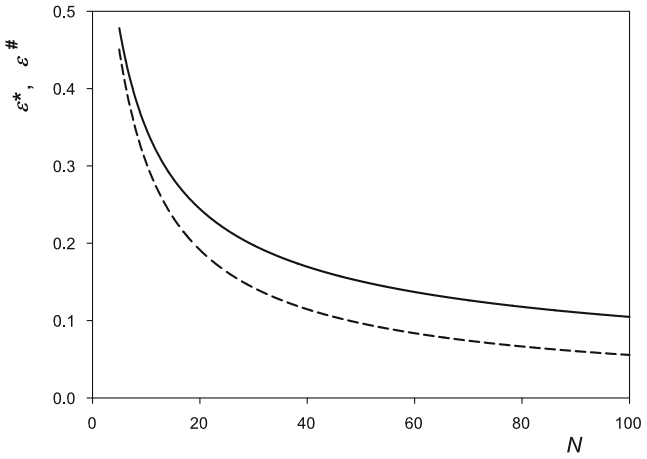

Fig. 5. Critical values of parameter ε versus number of particles N. Lower dashed curve: ε^* (one broken bond appears); upper solid curve: $\varepsilon^{\#}$, when potential well depths of both minima are equal.

2.3 Lattice rupture in harmonic approximation

In contrast to simulations at a constant loading rate [23,37,38,43], thermodynamics gives no answer on the kinetics of the lattice rupture. Nevertheless the estimation of time spans in both states can be done through the ratio of partition functions in the vicinity of one or other energy minimum, corresponding to the lattice state with equal bond lengths or one broken bond. This can be done as the partition function is proportional to the occupied phase volume. But the phase volume is proportional to the probability to stay in this state.

An accurate calculation of the partition function for the Morse lattice with one broken bond is quite a difficult task. But in the low temperature limit it can be done if the harmonic expansion $u(\ell) \sim \frac{1}{2}g\ell^2$ of the Morse potential is used; $g = u''(\ell) = 2\exp(-\ell)[1-2\exp(-\ell)]$ accounts for the stiffness of the Morse potential. There are three stiffness coefficients: one ($g_0 = u''(\ell_0)$) is for the lattice with all equal bond lengths; the two other stiffnesses g_1 and g_2 correspond to bond lengths ℓ_1 and one broken bond ℓ_2 in the disrupted state.

The major contribution to the total partition function for the lattice with one broken bond $Z_0 = \int d\Gamma \exp(-\widetilde{U}/T)$ at low temperatures gives phase volumes in the vicinities of potential energy minima, as the system is located mainly in one or the other minimum. Then the partition functions can be evaluated taking into account only these regions. Initially we consider the case of small elongations ($\varepsilon < \varepsilon^*$) when the only ground state minimum U_g of the lattice is that with equal bond lengths. The potential energy in the harmonic approximation can be expressed as

$$U \approx U_g + g_0/2\sum_{i=1}^{N+1}(x_i - x_{i-1})^2, \tag{22}$$

with $U_g = (N+1)[1-\exp(-\ell_0)]^2$. The partition function Z (up to an unessential factor) is

$$Z = \frac{\exp(-U_g/T)}{\sqrt{(N+1)(g_0/T)^N}};\qquad (k_B = 1). \tag{23}$$

The second energy minimum should be accounted in the case when $\varepsilon > \varepsilon^*$. The contributions to the partition function from every of $N+1$ minima are

$$\widetilde{Z} = \frac{\exp(-\widetilde{U}_g/T)}{\sqrt{1+N(g_1/g_2)\,(g_1/T)^N}}, \tag{24}$$

where $\widetilde{U}_g = N[1-\exp(-\ell_1)]^2 + [1-\exp(-\ell_2)]^2$.

Thus, taking into account that there can be $(N+1)$ minima, one has an approximate expression for the total partition function Z_0 for the lattice when it can be in one or the other state:

$$Z_0 = Z + (N+1)\,\widetilde{Z}. \tag{25}$$

One also can get an expression for the entropy in the low temperature limit (weak anharmonicity):

$$S = N \ln T + \ln(Z + \widetilde{Z}) + \frac{1}{T}\,\frac{U_{\rm g} Z + \widetilde{U}_{\rm g}\widetilde{Z}}{Z + \widetilde{Z}}. \tag{26}$$

Expressions (24)–(26) should be used with care: if ε is close to ε^* then the minimum corresponding to the disrupted state becomes very "soft" – one of the eigenvalues is close to zero, the vibrational amplitudes are very large and the harmonic approximation is inapplicable.

At low temperatures the system spends more time in the vicinity of one or the other minimum, but thermal fluctuations are still able to trigger the transitions between both states. The ratio of partition functions $Z/\widetilde{Z}$ gives the ratio of time spans $t/\widetilde{t}$ in each of them. From (23) and (24) the ratio $t/\widetilde{t}$ is:

$$t/\widetilde{t} = \exp\left(\frac{U_{\rm g} - \widetilde{U}_{\rm g}}{T}\right)(N+1)^{3/2}\left(\frac{g_0}{g_1}\right)^{N/2}\left[1 + N\frac{g_2}{g_1}\right]. \tag{27}$$

For the particular case when the potential well depths for the ground and "broken" minima are equal ($\varepsilon = \varepsilon^{\#}$ and $U_{\rm g} = \widetilde{U}_{\rm g}$), the ratio $t/\widetilde{t}$ does not depend on the temperature and, according to (27), is $t/\widetilde{t} \approx 0.12$ for $N = 10$. This ratio differs from unity due to the different statistical weights of these states.

MD simulations of reversible transitions between different states of the lattice are done using the canonical ensemble when an interaction with the heat bath is modeled by Langevin forces. Thermal fluctuations give the possibility for such transitions. The stochastic MD equations are

$$\frac{d^2 x_i}{dt^2} = -\frac{\partial U}{\partial x_i} + \mathcal{F}_i\,; \qquad (i = 1, 2, \ldots, N), \tag{28}$$

where $\mathcal{F}_i = \xi_i - \gamma \dot{x}_i$ are Langevin forces acting on every particle with friction γ and spectral properties $\langle \xi_i(t) \rangle = 0$ and $\langle \xi_i(t_1)\,\xi_j(t_2) \rangle = 2\gamma T \delta_{ij}\,\delta(t_1 - t_2)$; U is defined in (3). In MD simulations the random values $\{\xi\}$ depend on the integration step h, and are chosen from the uniform random distribution on the interval $\left[-\sqrt{6\gamma T/h}, \sqrt{6\gamma T/h}\right]$.

The special case $\varepsilon = \varepsilon^{\#}$ is considered for illustration, when potential well depths are equal for the states with equal bond lengths and one broken bond. It is convenient to consider the mean value of squared multidimensional distance from the state with all equal bonds: $\langle R^2(t) \rangle_\tau = \tau^{-1} \sum_{k=1}^{N} \int_t^{t+\tau} [x_k(t') - k\,\ell_0]^2\,dt'$ averaged over a time interval τ; $k\ell_0$ is the coordinate of the kth particle for the lattice with all equal bond lengths in equilibrium,

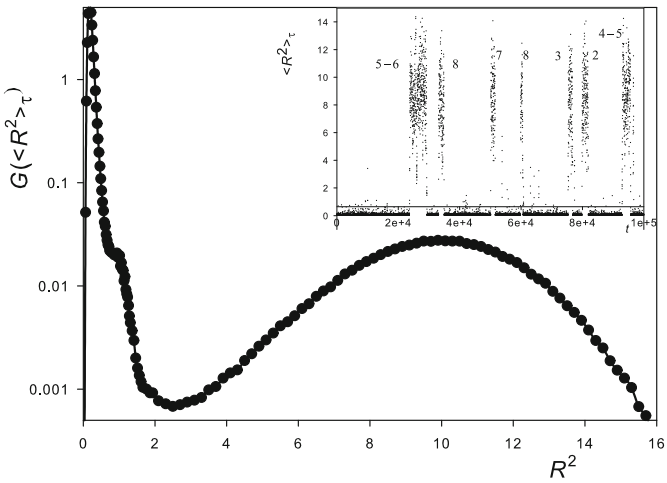

Fig. 6. Distribution function $G(\langle R^2 \rangle_\tau)$ of a squared distance from the ground minimum at specific elongation $\varepsilon^{\#}$. Averaging over $\tau = 5$. Temperature $T = 0.0125$. Barrier height separating minima $E^{\#} = 0.0193$. The ratio of areas is equal to the ratio of time spans and is 0.16 ± 0.07. A log-linear scale is used. Inset: the temporal behavior of $\langle R^2 \rangle_\tau$. Numbers show the number of ruptured bonds. Statistical processing of these data gives the distribution function $G(\langle R^2 \rangle_\tau)$. Time unit $[t] = \sqrt{2m/(C\alpha)}$ of potential (1).

and summation runs over all particles. $R^2_{\rm cr} \approx 2.5$ is the critical value, corresponding to the maximum of a barrier separating two energy minima. If $\langle R^2(t) \rangle_\tau < R^2_{\rm cr}$ then the lattice has (on average) equal bond lengths, and if $\langle R^2(t) \rangle_\tau > R^2_{\rm cr}$ then one or the other bond is broken at instant of time t.

The distribution function $G(\langle R^2 \rangle_\tau)$ normalized to unity is shown in Figure 6. This function has a high and narrow maximum near zero, corresponding to all equal bond lengths, and a wide maximum ($\langle R^2(t) \rangle_{\rm max} \approx 10$) for the state with one broken bond (accurate value from (19) is $\langle R^2(t) \rangle_{\rm max} = 10.1$). Actual values of $\langle R^2(t) \rangle_\tau$ are shown in the inset of Figure 6. The values of $\langle R^2(t) \rangle_\tau$ are at time instants $t = j\,\tau$ ($j = 0, 1, \ldots, 10^6$) averaged over the time interval $\tau = 5$.

The ratio $t/\widetilde{t}$ is the ratio of areas under the curve $G(\langle R^2 \rangle_\tau)$ separated by the value $R^2_{\rm cr} = 2.5$. MD simulations give $t/\widetilde{t} = 0.16 \pm 0.07$ at temperature $T = 0.0125$ and $t/\widetilde{t} = 0.15 \pm 0.05$ at $T = 0.015$ with standard errors large because of large fluctuations (compare with the accurate value $t/\widetilde{t} \approx 0.12$ obtained from (27)).

2.4 An example: cis-trans isomerization

Cis-trans isomerization plays significant role as one of fundamental chemical processes and has wide application in organic and bioorganic chemistry [60]. And as an example of our previous results we consider the particular, significant case of cis-trans isomerization where the rotation around one or other "single" bond is possible (see Fig. 7).

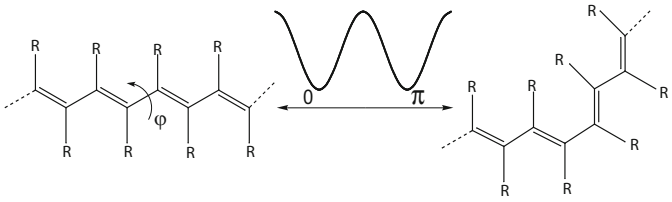

Fig. 7. Cis-trans isomerization of a polyene. Left: all trans-form of polyene; right: rotation by $\varphi = \pi$ gives cis-form. Energy profile of the reaction with $0 \leq \varphi \leq \pi$ is also shown. R is some or other chemical group.

For this case the Hamiltonian in its simplest form reads

$$H = \sum_{i=1}^{N} \frac{1}{2} J \dot{\varphi}_i^2 + U(\varphi_{i-1} - \varphi_i), \qquad (29)$$

where J is the moment of inertia of the unit cell (–RC=CR–), φ_i displacement of ith angle from its equilibrium value, and $U(\varphi_{i-1} - \varphi_i)$ – potential energy depending on the relative difference of neighboring angles. In (29) we assume fixed values of bond lengths and valent angles and the only degrees of freedom are torsional angles.

Potential energy in (29) depends on difference of angles $(\varphi_{i-1} - \varphi_i)$ and often is represented as $U(\varphi_{i-1} - \varphi_i) \sim A\{1 - \cos[2(\varphi_i - \varphi_{i-1})]\}/2$, where $(\varphi_i - \varphi_{i-1}) = 0$ corresponds to all trans-isomer, and $(\varphi_i - \varphi_{i-1}) = \pi$ to cis-isomer (see Fig. 7); A is the barrier height separating cis- and trans-isomers. This formulation allows to use results for the lattice rupture to the problem of cis-trans isomerization. Actually masses should be substituted by moments of inertia and Cartesian coordinates by torsional angles. Then (29) formally coincides with the lattice Hamiltonian (3).

An equilibrium between all-trans and cis-isomers is possible in some cases [61–63] and we also assume the equivalence of the ground state energies in cis- and trans-forms ($U_g = \widetilde{U}_g$). As discussed, the ratio of volume fractions of trans- and cis-isomers c_{trans}/c_{cis} in equilibrium is equal to the ratio $t/\widetilde{t}$ (27) with the corresponding choice of N and torsional angle stiffnesses. Torsional angle stiffnesses in all trans- (g_0) and cis-form (g_2 for the angle subjected to rotation by π and g_1 for other angles) can differ in the general case.

The ratio $t/\widetilde{t}$ depends on the ratios between torsional angle stiffnesses g_0/g_1, and g_2/g_1, and also on N (see (27)). If $g_0/g_1 \geq 1$ then $t/\widetilde{t}$ increases very rapidly with the growth of N. A more interesting case is when the torsional angle stiffness increases in the cis-form and $(g_0/g_1 < 1)$. Then equation (27) shows both increasing $(\propto N^{3/2})$ and decreasing $(\propto (g_0/g_1)^{N/2})$ contributions to the dependence on N. The last multiplier in (27) makes much less influence. The ratio c_{trans}/c_{cis} is shown in Figure 8 for two values of g_0/g_1. A rapid increase of c_{trans}/c_{cis} is observed at small N. Then this ratio has a maximum with height and position depending on g_0/g_1.

In the case when the ground state energies of trans- and cis-isomers are not equal $(U_g \neq \widetilde{U}_g$ in (27)) the major contribution to the relation of volume fractions c_{trans}/c_{cis} for small N gives the exponential factor $\exp\left[(U_g - \widetilde{U}_g)/T\right]$. But there exists essential contribution determined by the angle stiffnesses at large N. Thus the appealing assumption that the ratio $U_g/\widetilde{U}_g$ provides a major contribution to the relation c_{trans}/c_{cis} may cease to be valid in some cases.

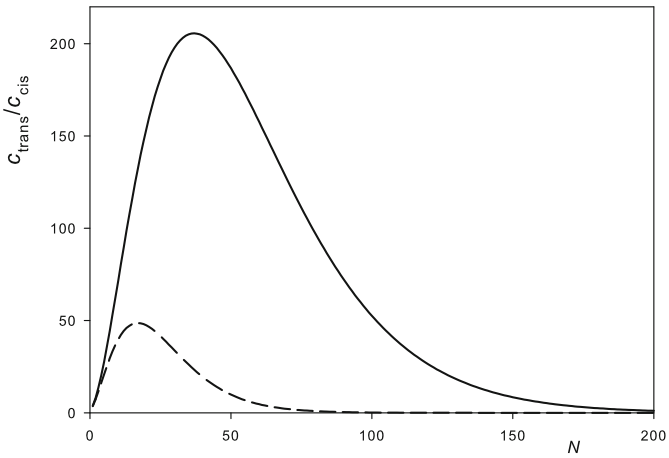

Fig. 8. Ratio c_{trans}/c_{cis} versus N for two values of the ratio g_0/g_1: $g_0/g_1 = 0.9$ (solid line) and $g_0/g_1 = 0.8$ (dashed line).

3 Conclusion

The thermodynamics of the Morse lattice rupture has been considered in the present paper. Expressions for the partition functions for the states with equal bond lengths and one broken bond are derived in the (quasi)harmonic approximation, when the anharmonicity effects can be neglected. The ratio of these partition functions gives an estimation for time spans in the ground and "broken" states. Lifetimes were also calculated using the canonical ensemble by MD-simulations. The results coincide within the statistical accuracy of MD-method. The method is illustrated for the case of cis-trans isomerization. Different behaviors are found depending on the torsional angle stiffness ratio of cis- and trans-isomers.

We thank S. Fugmann and I. Sokolov for discussions. The authors acknowledge the anonymous referee for criticism and helpful comments.

References

1. V.N. Likhachev, T.Yu. Astakhova, W. Ebeling, G.A. Vinogradov, Eur. Phys. J. B **72**, 247 (2009)
2. P. Schwaderer, E. Funk, F. Achenbach, J. Weis, C. Brúchle, J. Michaelis, Langmuir **24**, 1343 (2008)
3. T. Erdmann, S. Pierrat, P. Nassoy, U.S. Schwarz, Europhys. Lett. **81**, 48001 (2008)

4. Y.J. Sheng, S. Jiang, H.K. Tsao, J. Chem. Phys. **123**, 91102 (2005)
5. S.S. Sheiko, F.C. Sun, A. Randall, D. Shirvanyants, M. Rubinstein, H.-I. Lee, K. Matyjaszewski, Nature **440** (7081), 191 (2006)
6. S.A. Vanapalli, S.L. Ceccio, M.J. Solomon, Proc. Natl. Acad. Sci. USA **103**, 16660 (2006)
7. A.Y. Malkin, Polym. Sci. C **48**, 21 (2006)
8. V.C. Barroso, J.M. Maia, J. Non-Newton. Fluid Mechan. **126**, 93 (2005)
9. S.M. Bose, Y. Git, Macromol. Theory & Simulations **13**, 453 (2004)
10. Y.M. Joshi, M.M. Denn, J. Rheology **48**, 591 (2004)
11. M.C. Ritter, R. Jesudason, A. Majumdar, D. Stamenovic, J.A. Buczek-Thomas, P.J. Stone, M.A. Nugent, B. Suki, Proc. Natl. Acad. Sci. USA **106**, 1081 (2009)
12. L. Porter-Peden, S.G. Kamper, M.V. Wal, R. Blankespoor, K. Sinniah, Langmuir **24**, 11556 (2008)
13. H.-J. Lin, Y.-J. Sheng, H.-Y. Chen, H.-K. Tsao, J. Chem. Phys. **128**, 084708 (2008)
14. R.G. Haverkamp, A.T. Marshall, M.A.K. Williams, Phys. Rev. E **75**, 021907 (2007)
15. R.W. Welland, M. Shin, D. Allen, J.B. Ketterson, Phys. Rev. B **46**, 503 (1992)
16. A. Sain, C.L. Dias, M. Grant, Phys. Rev. E **74**, 046111 (2006)
17. D.R. Rottach, J.G. Curro, J. Budzien, G.S. Grest, C. Svaneborg, R. Everaers, Macromolecules **40**, 131 (2007)
18. D.L. Guzmán, J.T. Roland, H. Keer, Y.P. Kong, T. Ritz, A. Yee, Z. Guan, Polymer **49**, 3892 (2008)
19. E.M. Lupton, C. Nonnenberg, I. Frank, F. Achenbach, J. Weis, C. Brúchle, Chem. Phys. Lett. **414**, 132 (2005)
20. N. Yoshinaga, E. Kats, A. Halperin, Macromolecules **41**, 7744 (2008)
21. Y.-H. Lin, A.K. Das, J. Chem. Phys. **126**, 074902 (2007)
22. K. Eom, D.E. Makarov, G.J. Rodin, Phys. Rev. E **71**, 021904 (2005)
23. O.K. Dudko, G. Hummer, A. Szabo, Phys. Rev. Lett. **96**, 108101 (2006)
24. D. Panja, Phys. Rev. E **79**, 011803 (2009)
25. A. Politi, M. Zei, Phys. Rev. E **63**, 561071 (2001)
26. G. Meacci, A. Politi, M. Zei, Europhys. Lett. **66**, 55 (2004)
27. S. Ulrich, E. Buhler, J.-M. Lehn, New J. Chem. **33**, 271 (2009)
28. I.J. Lee, M. Yun, S.-M. Lee, J.-Y. Kim, Phys. Rev. B **78**, 115427 (2008)
29. C. Cavazzoni, R. Colle, R. Farchioni, G. Grosso, J. Chem. Phys. **128**, 234903 (2008)
30. J. Su, L. Zhang, J. Polym. Sci. B **46**, 370 (2008)
31. K.Wang, R.A. Zangmeister, R. Levicky, J. Am. Chem. Soc. **131**, 318 (2009)
32. H.-H.K.-B. Von Schmeling, Phys. Sol. State **47**, 934 (2005)
33. M.K. Beyer, H. Clausen-Schaumann, Chem. Rev. **105**, 2921 (2005)
34. M.J. Buehler, S. Keten, T. Ackbarow, Progr. Mater. Sci. **53**, 1101 (2008)
35. E.R. Hirst, Y.J. Yuan, W.L. Xu, Biosensors & Bioelectronics **23**, 1759 (2008)
36. C.H. Albrecht, H. Clausen-Schaumann, H.E. Gaub, J. Phys. Cond. Matt. **18**, S581 (2006)
37. O. Dudko, A. Filippov, J. Klafter, M. Urbakh, Proc. Natl. Acad. Sci. USA **100**, 11378 (2003)
38. H.-Y. Chen, Y.-P. Chu, Phys. Rev. E **71**, 010901(R) (2005)
39. M. Raible, M. Evstigneev, P. Reimann, F. Bartels, R. Ros, J. Biotechnol. **112**, 13 (2004)
40. H.A. Kramers, Physica (Amsterdam) **7**, 284 (1940)
41. P. Hänngi, P. Talkner, M. Borkovec, Rev. Mod. Phys. **62**, 251 (1990)
42. L. Bongini, R. Livi, A. Politi, A. Torcini, Phys. Rev. E **68**, 061111 (2003)
43. S. Fugmann, I.M. Sokolov, Phys. Rev. E **79**, 021803 (2009)
44. L. Bongini, R. Livi, A. Politi, A. Torcini, Phys. Rev. E **72**, 051929 (2005)
45. L. Bongini, L. Casetti, R. Livi, A. Politi, A. Torcini, Phys. Rev. E **79**, 061925 (2009)
46. L.S. Zarkhin, S.V. Sheberstov, N.V. Panfilovich, L.I. Manevich, Usp. Khimii **LVIII**, 644 (1989) (in Russian)
47. M. Takahashi, *Thermodynamics of One-Dimensional Solvable Models* (Cambridge Univ Press, Cambridge, UK. 1999)
48. T.Y. Astakhova, V.N. Likhachev, G.A. Vinogradov, Phys. Lett. A **371**, 475 (2007)
49. A.P. Chetverikov, W. Ebeling, M.G. Velarde, Eur. Phys. J. B **44**, 509 (2005)
50. N. Theodorakopoulos, M. Peyrard, R. MacKay, Phys. Rev. Lett. **93**, 258101 (2004)
51. R. Merkel, Phys. Rep. **346**, 343 (2001)
52. J.L. Lebowitz, J.K. Percus, Phys. Rev. **124**, 1673 (1961)
53. M. Pleimling, H. Behringer, Phase Transitions **78**, 787 (2005)
54. J. Dunkel, S. Hilbert, Physica A **370**, 390 (2006)
55. M. Costeniuc, R.S. Ellis, H. Touchette, B. Turkington, J. Stat. Phys. **119**, 1283 (2005)
56. V.N. Likhachev, T.Y. Astakhova, G.A. Vinogradov, Phys. Lett. A **354**, 264 (2006)
57. L.D. Landau, E.M. Lifshitz, *Statistical Physics*, 3rd edn. (Pergamon, Oxford, 1980)
58. M. Toda, *Theory of Nonlinear Lattices* (Springer-Verlag, Berlin, 1981)
59. A.P. Chetverikov, W. Ebeling, M.G. Velarde, Eur. Phys. J. B **70**, 217 (2009)
60. C. Dugave, L. Demange, Chem. Rev. **103**, 2475 (2003)
61. W.E. Von Doering, C. Sotiriou-Leventis, W.R. Roth, J. Am. Chem. Soc. **117**, 2747 (1995)
62. Q. Sui, D. Borchardt, D.L. Rabenstein, J. Am. Chem. Soc. **129**, 12042 (2007)
63. T. Shen, D. Hamelberg, J.A. McCammon, Phys. Rev. E **73**, 41908 (2006)